15th Australasian Fluid Mechanics Conference
The University of Sydney, Sydney, Australia
13-17 December 2004

Gravity currents in nature and industry

H. E. Huppert

Institute of Theoretical Geophysics
Department of Applied Mathematics & Theoretical Physics, University of Cambridge
CMS, Wilberforce Road, Cambridge CB3 0WA UK

Abstract

Gravity currents frequently occur in many natural and industrial situations. This article reviews the conceptual foundations used to understand and evaluate the evolution of gravity currents. Some of the latest results in specialised areas are highlighted. After an introduction, the paper ranges through the principal effects due to: low Reynolds number; compositional density differences; density differences due to dilute particulate matter; density differences due to concentrated particulate matter; and finally, the motion of a granular medium (with very little influence of the interstitial fluid). In addition, some effects due to permeable boundaries, rotation and propagation into an ambient which is either stratified or uniformly flowing will be considered.

Introduction

Gravity currents occur whenever fluid of one density flows primarily horizontally into a fluid of different density. (Predominantly vertical motion is described more naturally as plumes and involves different concepts [1].) There are numerous natural and industrial occurences of gravity current motions. These include: the spreading of honey on toast; the propagation of a relatively cold (and generally slightly wet) sea breeze, as happens so regularly on the East coast of Australia, across Canberra and at Perth (the Fremantle doctor); the outflow of the relatively warm and saline Mediterranean water through the Straits of Gibraltar into the Atlantic; the intrusion of giant umbrella clouds into the atmosphere following a volcanic eruption; and the flow of molten glass across a table to make sheet glass.

The first quantitative study of gravity currents was undertaken by von Kármán [2], who was asked by the American military to evaluate under what wind conditions poisonous gas released would propagate forward to envelop the enemy, rather than backwards to cause havoc to the troops who released the gas. Using Bernoulli's theorem, von Kármán showed that the velocity of the front, u, ahead of a layer of depth h, of relatively heavy fluid with density excess $\Delta\rho$ over that of the atmosphere ρ_o was given by

$$u/(g'h)^{1/2} = Fr, \qquad (1.1)$$

where the reduced gravity $g' = \Delta\rho g/\rho_o, g$ is the acceleration due to gravity and the Froude number, Fr, was evaluated by von Kármán to be $\sqrt{2}$. This is the condition to be applied at the nose of a current propagating at high Reynolds number $Re = uh/\nu$, where ν is the kinematic viscosity.

Such was the reputation of von Kármán that (1.1) and the paper in which it appeared quickly became celebrated, even though von Kármán had not considered the effects of wind in the atmosphere or pointed out that in a particular situation (1.1) is but one equation for the two unknowns u and h. Benjamin [3] revisited the problem and argued that von Kármán had used Bernoulli's theorem incorrectly (by taking a contour through a turbulent region) and rederived (1.1) by the use of a momentum integral, or flow force as Benjamin called it. Benjamin expressed surprise that he obtained the same result as von Kármán, and was clearly somewhat distressed by this. However, given that the starting point of both scientists was an (admittedly different) integral of the Euler equations, there was not any possibility that they could have arrived at a different result. In addition, since u, g' and h are the only variables in the (time-independent) problem, the non-dimensional quantity $u/(g'h)^{1/2}$ has to be a constant.

Expression of (1.1) has been used in (almost) all studies of gravity currents propagating at high Reynolds number as a form of conservation of momentum. Gravity currents propagating at low Reynolds number, behave quite differently, and, indeed, are not generally controlled at the front at all.

The next section briefly reviews the approach to studying low Reynolds number gravity currents, before continuing the above development for high Reynolds number currents, including the effects of particulate matter, permeable boundaries, rotation, intrusion into an ambient and, finally, the collapse of granular columns. The material is biased towards areas I have been involved with and know best. I hope this stance is understandable, though it means that a number of important contributions have not been mentioned.

Viscous Gravity Currents

Viscous gravity currents propagate under a balance between viscous and buoyancy forces. In all problems so far solved the viscous fluid has been assumed to spread as a thin layer and the concept of lubrication theory has been appropriate. Thus the velocity profile is parabolic and conservation of mass leads to a governing partial nonlinear differential equation in space and time for the unknown free surface height $h(\mathbf{x}, t)$ as depicted in figure 1. Thus, for example, for a current spreading along

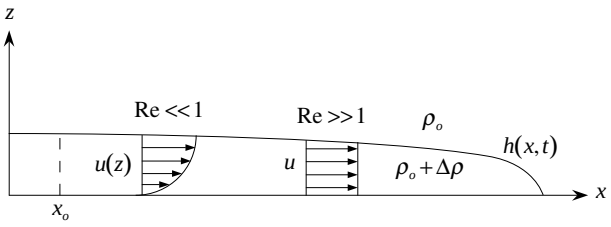

Figure 1: A sketch of a propagating gravity current showing the notation and parabolic velocity profile for $Re << 1$ and the uniform velocity profile for $Re >> 1$.

a horizontal base in either a wide channel or an axisymmetric situation, the governing equation is [4]

$$\frac{\partial h}{\partial t} - \frac{\beta}{x^n}\frac{\partial}{\partial x}\left(x^n h^3 \frac{\partial h}{\partial x}\right) = 0, \qquad (2.1)$$

where $\beta = \frac{1}{3}g/\nu$, $n = 0$ in cartesian coordinates and $n = 1$ in radial coordinates (where x is interpreted as the radius), under the assumption that the Bond number $B = T/\rho l^2 << 1$, where T is the surface tension and l some typical horizontal length, so

that surface tension effects along the interface and nose can be neglected. To the governing equation (2.1) must be added an overall volume conservation relationship of the form

$$\int_o^{x_N(t)} (2\pi x)^n h(x,t)dx = qt^\alpha, \tag{2.2}$$

where $x_N(t)$ is the extent of the current and the volume is assumed to be qt^α, where, for example, $\alpha = 0$ represents a constant volume current and $\alpha = 1$ a current fed at constant flux.

A similarity form of solution is easily obtained for (2.1) and (2.2) and is written as [4,5],

$$h(\mathbf{x},t) = \zeta_N^{2/3}(q^{2-n}/\beta)^{1/(5-n)} t^{[(2-n)\alpha-1]/(5-n)} \Phi(\zeta/\zeta_N), \tag{2.3}$$

where the similarity variable

$$\zeta = \left(\beta q^3\right)^{-1/(5+3n)} x t^{-(3\alpha+1)/(5+3n)}, \tag{2.4}$$

$\zeta_N(\alpha,n)$ is determined by (2.2) and $\Phi(w)$ satisfies the singular nonlinear differential equation

$$\left(w^n\Phi^3\Phi'\right)' + \frac{(3\alpha+1)}{(5+3n)} w^{1+n}\Phi' -$$

$$\frac{1}{(5-n)[(2-n)\alpha-1]} w^n\Phi = 0 \tag{2.5}$$

$$\Phi(1) = 0. \tag{2.6}$$

The similarity variable (2.4) indicates immediately, with no further analysis, that the extent of the current is given by

$$x_N = \zeta_N \left(\beta q^3\right)^{1/(5+3n)} t^{(3\alpha+1)/(5+3n)}. \tag{2.7}$$

Experimental results for the rate of propagation of such viscous spreading are in excellent agreement with the theoretical determination [4-7]. The motivation for the original study was the availability of wonderful data on the spreading of the lava dome formed in the crater of the Soufrière of St Vincent in the West Indies after the eruption of 1979. The resultant lava dome slowly increased in volume, and spread horizontally for five months across the crater floor, by which time the pancake-shaped dome had a height of 130m, a mean diameter of 870m and a volume of $5\times10^7 m^3$ [8]. Observations of the volume then indicated that $\alpha = 0.66$, which should lead to a radial time dependence, from (2.7), of $(3\alpha+1)/8 = 0.37$, in good agreement with the measured value of 0.39. In addition, (2.7) can then be inverted to determine the reasonable value for the kinematic viscosity of $6\times10^7 m^2 s^{-1}$. Considerable further work has been done to extend this initial model in order to be more realistic by including the effects of compressibility of the interstitial gas in the magma [9], and solidification of the thin upper carapace of the lava dome [10,11]. The theoretically determined shape, (2.3) has also been successfully used to describe the shape of the numerous lava domes recently observed on Venus [12].

The flow at low Reynolds number of a viscous fluid down a slope occurs in many different situations: the splattered wet mud down a car windscreen; liquid detergent on a slanted plate; and rainwater down the roof of a glass conservatory. A fundamental problem, which has acted as the foundation of further studies, is whether a broad band of viscous fluid, uniform in depth across the slope, can continue to flow in a fashion independent of the cross-slope coordinate. This situation was first considered by Huppert [6] who showed, again under the assumption that $B << 1$, that there is a parabolic velocity profile and that the free surface $h(x,t)$ is governed by

$$\frac{\partial h}{\partial t} + (g\sin\theta'/\nu)h^2\frac{\partial h}{\partial x} = 0, \tag{2.8}$$

where x is the coordinate down the slope, which is inclined at angle θ to the horizontal. By use of either the theory of characteristics or by similarity theory, Huppert showed that the appropriate theoretical solution of this two-dimensional flow was

$$h = (\nu/g\ \sin\theta)^{1/2}\ x^{1/2}\ t^{-1/2} \tag{2.9a}$$

for

$$0 \le x < x_N = \left(9A^2 g\ \sin\theta/4\nu\right)^{1/3} t^{1/3}, \tag{2.9b}$$

where A is the initial cross-sectional area of the current. The relationship (2.9a) indicates that at any time the free surface increases in thickness down the slope like the square root of the coordinate down the slope until the point $x = x_N$ at which point the current ends (abruptly in this solution that neglects surface tension) and that at any point down the slope, once the current has passed overhead, its thickness decreases like the square root of time.

To test the validity of this theoretical prediction, Huppert conducted a series of experiments with different viscous fluids flowing down slopes of different angles to the horizontal. Initially the motion was virtually independent of the cross-slope coordinate and in good agreement with the predictions of (2.9). However, after some time the flow front spontaneously developed small amplitude waves of fairly constant wavelength across the slope. The amplitude of the waves increased in time as the maxima (point furthest down the slope) travelled faster than the minima. The wave length remained unaltered. For silicon oils the subsequent shape was a periodic, triangular front with tightly rounded maxima, connected by very straight portions at an angle to the slope, to extremely pointed minima. For glycerine, the shape was also periodic, though with much less tightly rounded maxima, again connected by extremely straight portions, almost directly down the slope, to very broad minima. To my knowledge no other shape has been seen for different fluids. The initial instability is due to the effects of surface tension, which were neglected in the two-dimensional analysis. Incorporating these effects at the tip, Huppert was able to show that the wavelength of the instability was well represented by

$$\lambda = \left(7.5A^{1/2}T/\rho g\sin\theta\right)^{1/3}, \tag{2.10}$$

independent of the co-efficient of viscosity, which only sets the timescale of the instability and its onset.

Compositional Currents

In (almost) all situations, very soon after release, a current whose density difference is due to a dissolved component, such as salt, so that the density is conserved, propagates in such a way that its horizontal extent is very much larger than its vertical extent. Under the assumption that the Reynolds number is large, the balance is then between inertial and buoyancy forces and standard shallow water theory [13] can be applied. Alternatively, Huppert and Simpson [14] introduced the concept of a "box model", which considers the simple model that results from assuming the current to evolve through a series of equal area rectangles, or equal volume cylinders, as appropriate, with no variations of any properties in the horizontal. (An integral justification of this approach is given in [15]). This approach leads immediately to the relationship

$$x_N = C(Fr)(g'A)^{(2-n)/6} t^{(4-n)/6}, \tag{3.1}$$

where C(Fr) is dependent only on the Froude number and A is the cross-sectional area in two dimensions (n=0) and the volume in three dimensions (n=1) of the current. Even if mixing occurs the product $g'A$ remains constant, and equal to the initial value.

The use of similarity theory [16-18] leads to a relationship which differs only in the premultiplicative constant in (3.1), and then only by a relatively small quantitative amount. (But that is the power of the correct dimensional constraints!)

Entrainment of ambient fluid into the flow has been investigated both theoretically and experimentally [19,20] by following the intrusion of an alkaline current into an acidic ambient. Entrainment takes place almost entirely at the head of the current owing to shear instabilities on the interface between the current and the ambient and by the over-riding of the (relatively less dense) ambient fluid as the head propagates over it. An entrainment or dilution ratio E, defined as the ratio of the volumes of ambient and original fluid in the head, which hence must be non-negative, can be shown by dimensional analysis, and was confirmed by experiment, to be independent of g', and to be given in two dimensions by $E = [1 - c_1 y_N / A_s^{1/2}]^{-c_2} - 1$, where A_s is the cross-sectional area of fluid in the head at the end of the slumping phase (which occurs before the current has propagated about 10 lock lengths), y_N is the position of head beyond the slumping point [14], and $c_1 \approx 0.05$ and $c_2 \approx 1.5$ are empirical constants determined by the roughness of the floor.

Particulate-laden Currents

When heavy (or possibly relatively less dense) particles drive the flow the major new addition to the advective effects is that the particles fall (or rise) out of the flow and the driving buoyancy continually decreases. Examples of this form of motion are the terrifying flows seen in lower Manhattan on September 11 and the awesome hot, ground-hugging pyroclastic flows which can be the life-threatening, destructive result of volcanic eruptions such as occured recently at Pinatubo in Indonesia, Unzen in Japan and Montserrat in the Caribbean. After a sufficient number of particles have dropped to the ground, so that the bulk density of this hot flow is no longer greater than that of the surrounding atmosphere, the current can suddenly rise quite dramatically, taking much particulate matter high into the atmosphere.

The approach most frequently taken to analyse the sedimentation if the concentration is not too large is to assume that the (high Reynolds-number) flow is sufficiently turbulent to maintain a vertically uniform particle concentration in the main body of the current. However, at the base of the flow, where the fluid velocities diminish appreciably, the settling of particles occurs at the (low-Reynolds-number) Stokes velocity V_s in otherwise quiescent fluid. Quantitatively, this indicates that, neglecting particle *advection* for the moment and assuming that the particles are all of one size, if N_p (which is possibly a function of time and position) denotes the total number of particles per unit horizontal area in a layer of depth h, the change of N_p in time $\delta t, \delta N_p$, due only to the sedimentation, is given by $\delta N_p = -V_s C_0 \delta t$, where C_0 is the (number) concentration (per unit volume) just above the base of the flow. Vigorous turbulent mixing implies that $C_0 = N_p/h$, which (on taking the appropriate infinitesimal limits) indicates that $dN_p/dt = -V_s N_p/h$, a relationship which has been carefully verified by experiments [21]. Incorporation of advection of particles by the mean flow then results in

$$\frac{D}{Dt}\phi \equiv \frac{\partial \phi}{\partial t} + \mathbf{u}.\nabla\phi = -V_s\phi/h, \qquad (4.1)$$

where ϕ is the volume concentration of particles.

Shallow water equations incorporating (4.1) are easily derived [17,18]. There are no similarity solutions and recourse, in general, has to made to numerical solution. There is very good agreement between the numerical solutions and experimental determinations carried out specially to test them.

Aside from numerical solutions, it is also possible to develop asymptotic, analytic solutions based on the smallness of $\beta_S = V_S/(g'_o h_o)^{1/2}$, where g'_o is the *initial* reduced gravity of the system [15]. This is an example of the interesting problem which can be stated in general as the nonlinear partial differential equation

$$\mathcal{N}_1[\Phi(x,t)] = \varepsilon \mathcal{N}_2[\Phi(x,t)], \qquad (4.2)$$

where $\mathcal{N}_1$ and $\mathcal{N}_2$ are nonlinear operators in some spatial coordinate x and time t. For $\varepsilon \equiv 0$ there is a similarity solution to (4.2) and a special value of x, x_* say, such as that at the nose of the current, which increases continuously with time of the form $x_* = f(t)$. However, for $\varepsilon \neq 0$, no matter how small, (4.2) does not have a similarity solution and eventually, for sufficiently large t, x_* attains a constant. Thus, in the style of singular perturbation problems, for sufficiently large t the solution for $\varepsilon = 0$ departs by as much as you like from solutions for $\varepsilon << 1$. It must, on the other hand, be possible to obtain asymptotic solutions to (4.2) in a perturbative sense. Such a technique is constructed, in part, in [15].

When there is an external flow present, as originally put to von Kármán, the propagation of the current is significantly influenced, and in a different way if it is propagating with the ambient flow or against it. Hogg and Huppert [22,23] initiated an analysis and a series of laboratory experiments to investigate this case. They showed that in two dimensions the flow was dependent on the single non-dimensional parameter $\Lambda = UA/(l_\infty^2 V_S)$, where U is the effective mean external flow experienced by the current (shown in [22] to be 0.6 times the actual current), A is the cross-sectional area (or volume per unit width) of the fluid instaneously released at the base of the flow, the reduced gravity of the particles of density ρ_P is given by $g'_P = (\rho_P - \rho_a)g/\rho_a, \rho_a$ is the density of the ambient and $l_\infty = (g'_P)\phi_o A^3/V_s^2)^{1/5}$. The parameter Λ represents the ratio of the mean external velocity to the settling velocity of the particles. When Λ is small, (little effect of the flow in the ambient) the flow is roughly the same upstream or downstream. As Λ increases the effects of the flow in the ambient increase and the upstream flow is considerably restricted. However, even for large Λ there will still be some upstream propagation—much to the disbelief and then dismay of the government official who asked me to carry out this work in order to show that a new dredging technique which removed sand from the bottom of the harbour, by blowing high velocity water at it, would be totally removed by the outgoing tidal flow and not propagate at all upstream across the harbour and contaminate the highly valuable stocks of fish and oysters there! Figure 2 presents the theoretically determined maximum non-dimensional upstream distance of a particulate intrusion in a uniformly flowing ambient as a function of Λ and the laboratory experimental data obtained using various size particles. The agreement shown is excellent; and one of the best I have ever obtained in my career, and hence my pleasure with it.

Extensions of this idea to an axisymmetric (rather than line) source are summarised in [24,25] where the relevant parameters and shape of the current are carefully discussed. My clever graduate student, Anja Slim, [26] is also working in this area for her Ph.D. and has already developed a number of results with the final aim of understanding the details of how an initially vertically penetrating, particulate-rich, volcanic eruption column is

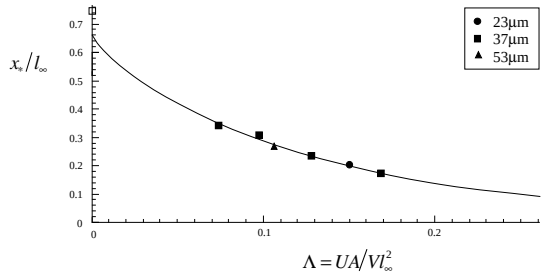

Figure 2: The theoretical prediction and experimental data of the maximum nondimensional upstream penetration of a particulate gravity current in a uniform flowing ambient, x_*/l_∞, as a function of $\Lambda = UA/(V_S l_\infty^2)$ for three different particle sizes.

influenced high in the atmosphere by the prevailing winds.

Further details of some of this work can be found in [27].

Additional Effects

The preceding four sections have detailed some of the fundamental relationships for the propagation and evolution of a gravity current. Many other special effects are possible. We will describe some of these under the headings of: effects of a permeable boundary; intrustion below a stratified ambient; and effects of rotation.

Permeable boundaries

There are many natural and industrial situations where a gravity current flows over a permeable boundary and seeps into it. Examples include protecting liquid-containing structures by sourrounding them with a deep gravel bed, the seepage of tidal inflow up a beach and the everyday occurrence of honey seeping into toast. The most important new ingredient is that fluid from the current continuously seeps through the boundary, which reduces the volume of the current whose propagation must eventually cease.

The flow of the current at low Reynolds number was considered by Acton, Huppert and Worster [28]. The parabolic velocity profile in the current is augmented by a sink term in the local continuity equation which leads, in two dimensions, the only situation that has been investigated, to

$$\frac{\partial h}{\partial t} - \beta \frac{\partial}{\partial x}\left(h^3 \frac{\partial h}{\partial x}\right) = -(kg/\nu)(1+h/l), \qquad (5.1)$$

which takes the place of (2.1), where the term on the right hand side represents effects of the flow into the porous medium below, which is categorised by the intrinsic permeability of the medium k and l denotes the length of the current. In contrast to the situation for an impermeable boundary, (5.1) has a similarity solution only for the special case of $\alpha = 3$, for which the flux into the current at the origin just balances that out of the current through the permeable boundary. For other values of α solutions of (5.1) must be obtained by numerical integration. This was done by Acton *et al.* [28], who also carried out special experiments to compare observational data on the length of the current as a function of time with their numerical solution. The result, as shown in figure 3, resulted in an extremely good comparison, with a final run-out length which scales with $S_H = \left(A^2 k\right)^{1/3}$ for $\alpha = 0$. For $\alpha < 3$ all currents eventually stop; for $\alpha \geq 3$ all currents continue to propagate because the incoming flux overpowers the seepage. Note the similarity in concept between the slow loss of driving force due to seepage, considered here, and the loss of buoyancy due to slow particle fallout,

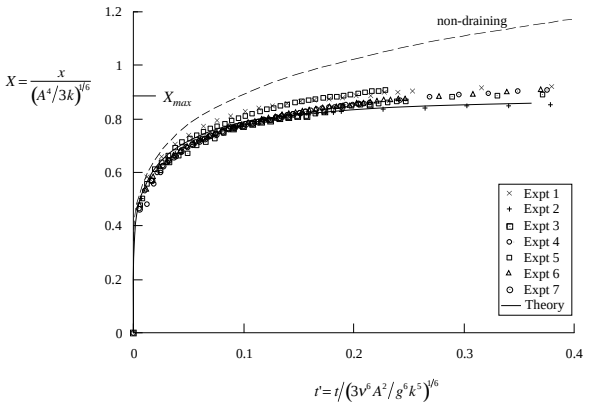

Figure 3: The nondimensional length of a low Reynolds number gravity current flowing over a permeable boundary as a function of the dimensionless time for seven different experiments. The solid curve is the theoretical prediction determined from numerical integration of (5.1) and the dashed line is the similarity solution for an impermeable boundary given by (2.7).

considered in Section 4. The general approach discussed there, as outlined in [15,29] has not been applied to this area, though it no doubt could be done so fruitfully.

When the current propagates at high Reynolds number the balance of forces are of course different, but the importance of seepage through the boundary is still paramount. This problem was initially considered by Thomas, Marino and Linden [30] and then extended by Ungarish and Huppert [31]. The latter solved numerically the shallow water equations governing mass and momentum for a two-dimensional geometry as well as obtaining analytical, box model solutions in both rectangular and axisymmetric geometries. This allowed closed form solutions for the extent of the current as a function of time and its final extent to be determined, which were in fair agreement with both the two-dimensional experiments carried out by Thomas *et al.* [30] and the numerical solutions.

Propagation under the base of a stratified ambient

In all the aforegoing discussion, it has been assumed that the ambient is homogeneous and not influenced in any way, in particular set into motion, by the intruding current. However, in both the atmosphere and in the oceans the ambient is stratified; and it immediately raises the question of why the solutions so far obtained are applicable in these more complicated, natural situations—or has something important been left out? What clearly has been left out of the homogeneous models is the possibility of exciting internal waves in the ambient by the propagation of the current. Viewed from another angle, the question that needs considering is what fraction of the potential energy stored in the original (unstable) buoyancy distribution is lost to the internal wave motion, in contrast to that which is put into the kinetic energy of motion and that which is dissipated. The first investigation of the influence of a stratified ambient was presented by Maxworthy *et al.* [32]. They investigated the propagation of a saline current below a linearly stratified saline ambient in a rectanglular container. Their study was a combination of laboratory and numerical experiments. The numerical solutions, obtained from a full Boussinesq formulation, were in very good agreement with their measurements. They focused attention on the speed of propagation of the nose during the initial stage only, for which a good agreement between theory and numerical computation was obtained. Ungarish and Huppert [33] then extended this investigation by determining appropriate an-

alytical solutions. Using the methods of characteristics on the non-linear shallow water equations, which neglects the influence of waves in the ambient, they were able to obtain solutions for the front velocity as a function of the parameter S, defined as the ratio of the density difference between the fluid that makes up the bottom of the ambient and that at the top to the density difference between the fluid of the incoming current and that at the top. The results of their calculations, compared with the Maxworthy *et al*. experimental results, makes up figure 4.

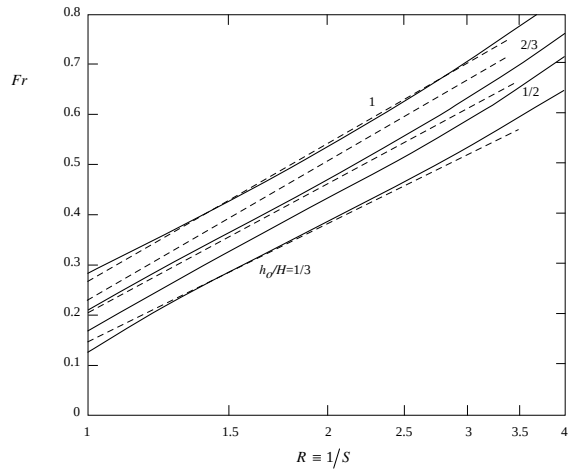

Figure 4: The Froude number, as a function of the logarithm of the inverse stratification parameter S for a high Reynolds number gravity current propagating beneath a stratified ambient for different initial depth ratios. The theoretical evaluation of Ungarish and Huppert [105], represented by the solid curves, are compared with the experimental results suggested by Maxworthy *et al* [32], represented by dashed curves

Ungarish and Huppert are currently considering how to incorporate the effects of stratified waves in the ambient. They intend first to solve a linear leewave model coupled to a deforming current and thereby evaluate the amount of energy that has gone into the waves. At the same time, they are carrying out laboratory experiments in which an array of conductivity probes will allow a direct sampling of the wave displacements in the ambient, from which, using sophisticated processes in signal analysis, the energy given up to the waves in the ambient will be determined as a function of S and the geometry of the container—a wave guide if $l >> H$, the depth, and an effectively infinite medium into which the waves can radiate away if $l << H$.

Some effects of rotation

Rotational effects, which can be dominant, for example, in rapidly rotating systems in the laboratory, in industrial machines or due to the rotation of the Earth, brings in the initially counter-intuitive effect that fluid flows at right angles to the pressure gradient, in analogy with at least my experience of life, where you push in one direction and the result goes off in another—a concept which the naive, inexperienced young never understand! The effect of rotation on gravity currents can be particularly powerful in the presence of a boundary because a pressure gradient into the wall can easily be set up and drive a current which hugs the boundary [34]. These situations have been reviewed in detail by Griffiths [35].

An experimental investigation of axisymmetric gravity currents, where boundaries play no role, was carried out at the large rotating system housed in the Coriolis laboratory at the Laboratoire des Ecoulements Geóphysiques et Industriales, Grenoble by Hallworth, Huppert and Ungarish [36]. The major new feature of the results was the attainment of a maximum radius of propagation, attained in about one third of a period of revolution, in contrast to some theories which, totally unjustifiably, assume from the outset that the motion goes on for many rotation periods before anything interesting happens. The observed result had been predicted earlier by a theoretical investigation of the governing shallow water equations by Ungarish and Huppert [37], who evaluated that $r_{max} \approx 1.6\mathcal{C}^{1/2}$, where $\mathcal{C} = \Omega_o/(h_o g')^{1/2}$, Ω is the rotation rate of the instrument and the initial dense fluid, of reduced gravity g' was initially contained in the cylinder of radius r_o and height h_o. Thereafter the motion in the fluid consisted of a contraction/relaxation/propagation of the current with a regular series of outwardly propating pulses. The frequency of these pulses was observed to be slightly higher than inertial, independent of h_o and g', with an amplitude of the order of magnitude of half the maximum radius, as shown in figure 5.

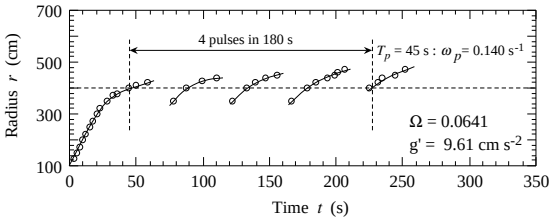

Figure 5: The radius of the leading edge of successive outward propagating fronts as a function of time for gravity currents intruding into a homogeneous, rotating ambient.

Concentrated Flows: Mud, Slurries and Landslides

As the concentration of particles increase, the statement of low concentration employed in driving (4.1) on the assumption that each particle sediments with its independent Stokes freefall speed V_s becomes less reliable. New effects must enter; and indeed, as the concentration becomes very high this situation relates more to mud flows than to the motion of suspended particles. Partly to investigate this problem, Hallworth and Huppert [38] carried out a systematic series of experiments on the instantaneous release of two-dimensional, heavy particle-driven gravity currents down a channel. Relatively low concentrations, with initial volume concentrations ϕ_o in the range $0 < \phi_o < 0.275$ were well described by the numerical solutions of (4.1) or the analytical box models associated with it, with the final runout length of the sedimented deposit increasing with ϕ_o. Beyond this critical initial volume fraction of particles, the resulting dense current came to an abrupt halt at some point down the channel, depositing the bulk of its sediment load as a relatively thick layer of fairly constant thickness, characterised by a pronounced, steep snout. A very much thinner layer of sediment extended for some distance beyond the arrest point. This layer was deposited from the subsequent propagation of a slower moving, low concentration residual cloud and the final runout length of the sediment layer decreased with increasing ϕ_o. This form of motion was observed for $0.275 < \phi_o < 0.45$, this upper limit being the approximate maximum for which Hallworth and Huppert were able to produce a fluid-like initial volume.

Over the last decade, for its obvious natural applications there has been considerable research to try to understand these high-concentration flows, exemplified by mud slides. Large mud flows can occur in mountainous regions after intense rains where they can move large boulders and even trees to cause enormous damage and loss of life and produce interesting al-

luvial fans. They also occur on submarine continental slopes, where they contribute to geomorphological evolution. There is hence considerable interest in both the geological and engineering community in such flows. Unfortunately, in contrast to all the work so far described in this article, for which it has been assumed that the constitutive relationship is Newtonian, it is quite definite that mud and the like are non-Newtonian. But how are they to be described? A plethora of rheological models have been proposed—power law, viscoplastic, Bingham plastic, Herschel–Bulkley,... Because of these different conceptual models, it is difficult to carry out systematic experiments which either test or verify any of these flows. Each person understandably views the possible contributions to the broad spectrum of science differently, but I find it unsatisfying working in areas where the fundamentals are on such shaky ground. Nevertheless, considerable activity has been shown in this area, which might be broadly and briefly summarised as follows.

The main new effect that enters is the possibility of a critical yield stress, τ_o, below which there is no shear possible in the flow. (There are similarities here to some of the models for non-Newtonian lava flows, nicely reviewed in [39].) This leads to a variety of features which are unknown in Newtonian fluids, even in quite simple situations. For example, a uniform layer of fluid mud can remain stationary on an incline, if the depth of the mud or the slope of the incline is sufficiently small. When motion does occur it is generally investigated under two approximations: either the flow is so slow that inertia is neglected (the more usual case); or so fast that a boundary-layer approximation is appropriate. A variety of different initial set-ups have been solved for the motion of the mud and its final shape on a horizontal surface, down an inclined plane and over a gently sloped conical surface, representing a shallow basin or hill [40, 41]. Much further work in this area needs to be done before a good scientific understanding has been obtained and the results can be applied to the all-important area of hazard assessment, with the potential to save hundreds of thousands of lives and millions of wasted dollars.

Granular flows

Partially motivated by recent interest in the flow of granular medium, my superb geological colleague, Steve Sparks, a student Gert Lube and I conducted a series of experiments in which various granular materials, initially contained in a vertical cylinder, were rapidly released onto a horizontal surface to spread out unhindered over it [42]. The materials were couscous, rice, dry sand, salt and sugar, all of which have different size and shape. The horizontal plane used was either wood, a smooth surface of baize lying on wood, a smooth transparent Plexiglas plane or a rough plane of sandpaper. The detailed spread of the granular material was independent of the explicit grains employed or the bounding surfaces. Eight different cylinders,in radius, r_i, from 1.7 to 9.7 cm, were used. Some experiments were recorded and later analysed on a digital high-speed video at 500 frames per second. After all motion had ceased, the profile of the resultant deposit was measured, to find the final runout radius, r_∞, central cone height, h_∞, and the steepest incline, α, of the upper surface.

For all values of the initial aspect ratio $a = h_i/r_i$, where h_i is the initial height of the granular medium, there was a central undisturbed cone of material which did not partake in the motion, whose angle was close to 60°, corresponding to an aspect ratio of 1.7. This can be interpreted as an internal friction angle for the material. At the base, three different regions were captured by video during the collapse: a stationary circular region, of radius r_i; a ring of previously deposited particles; and an outer ring of material which was still flowing. These last two regions were divided by a moving interface that propagated outwards until the flow front came to rest.

Observations from the high-speed photography indicate that other aspects of the motion naturally divide themselves into three different regimes dependent on a . For initial aspect ratios $a < 1.7$, the upper surface of the released material was divided into an inner stationary circle (which remained at the initial height, h_i) outside of which was flowing material. After the flow front had ceased propagating, a moving interface on the upper free surface appeared, which separated static from flowing particles and which propagated inward from the stationary front. For $a < 1$ the final deposit consisted of an inner, undisturbed central region beyond which there was an axisymmetric, tapering frontal region with α in the range of the angle of repose. For $1 < a < 1.7$ the avalanching which occured after the flow front had stopped moving removed the undisturbed central region.

For $a > 1.7$ the entire upper surface flowed from the beginning of each experiment. Initially, the upper free surface remained undeformed and horizontal. After the column lost some height, deformation of the top occurred, to form a dome whose radius of curvature decreased with time. The final deposit had a steep central zone and an axisymmetric tapering frontal region with α less than the angle of repose.

A transition in behaviour of collapse was evident from the video analyses to occur when a exceeds about ten. Immediately upon lifting the container the entire free surface began to flow. A flow front developed at the base of the column and propagated outwards while removing material from the centre. In contrast to lower initial aspect ratios, the upper surface of the column remained undeformed until its height sank to that of the neighbouring flat frontal region. Also, once the flow at the base had ceased, an interface between moving and stationary material appeared on the upper free surface but propagated outward from the centre to the flow front. The value of α decreased monotonically with increasing a.

The quality of the observational data and the similarity of the results for the different materials suggest that, with the use of dimensional analysis, the data can be collapsed in a systematic way. The initial experimental set up is determined by r_i, a and g, the acceleration due to gravity. Our ability to collapse all the data using only this input, and not any material properties, is a robust test for the assumption that no additional material property, such as the friction between individual grains, is needed to describe the motion.

The difference between the initial and final radius, $\delta r = r_\infty - r_i$, must be expressible as $\delta r = r_i f(a)$. A plot of $\delta r/r_i$ makes up figure 6. For $a < 1.7$, because there is no motion of the inner region, the resultant expression must be independent of r_i, which requires that $f(a) \propto a$. From figure 6 we determine that the constant of proportionality which best fits the data is 1.3. For $a > 1.7$ the best fit power law to the data for all grains is given by $f(a) = 1.6a^{1/2}$.

The final height at the centre is similarly expressible as $h_\infty = r_i\eta(a)$. Figure 6 also presents all the data for h_∞/r_i as a function of a. For $a < 1.7$, $h_\infty = h_i$, and so $\eta(a) = a$, as indicated by the data. For $1.7 < a <$ c.10 the best fit power law to the data is given by $\eta(a) = 0.88a^{1/6}$. For $a >$ c.10 there is a clear indication that h_∞ decreases with increasing a. This is in response to the wave that originates from the centre and removes material outwards. Unfortunately, the data are a little too scattered to be quantitatively analysed with confidence.

So far the parameter g has not entered our expressions because

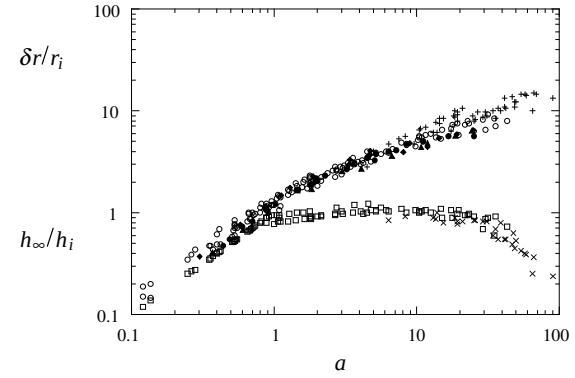

Figure 6: Nondimensional radial displacement and height at the centre of a pile of axisymmetric collapsing grains. Points marked with a cross are for experiments in which the cylinder was raised height H from the base before releasing the grains, and the aspect ratio is defined as $(H+h_i)/r_i$. This shows that in the final runout distance only maximum initial height is relevant (and initial radius).

it is the only input parameter for which time is involved in its dimensions, and $\delta r, h_\infty/r_i$ are both independent of time. The value of g will affect the total time for collapse, t_∞, which is defined as the time between the initiation of the experiment and that at which the flow front stops propagating. The high speed video allowed us to determine t_∞ reasonably accurately. By dimensions, it must be of the form $t_\infty = (r_i/g)^{1/2}\psi(a)$, for some function $\psi(a)$. A plot of $t_\infty/(r_i/g)^{1/2}$ as a function of a is presented in figure 7. As before, for $a < 1.7$, an expression independent of

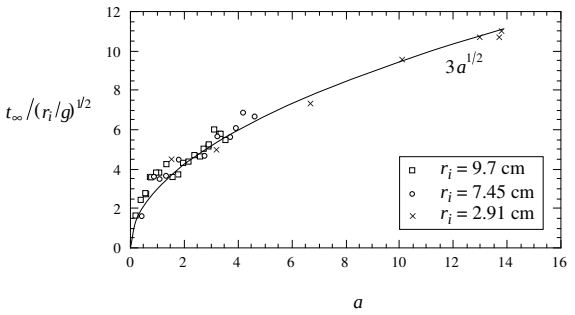

Figure 7: Nondimensional time until the grain front ceased motion as a function of a.

r_i requires $\psi(a) \propto a^{1/2}$, which is consistent with the data for a constant of proportionality of 3.8. For $a > 1.7$ the best fit power law through the data yields $\psi(a) = 3a^{1/2}$, which indicates that $t_\infty = 3(h_i/g)^{1/2}$. Note that the time taken for a particle to fall a height h_i under gravity is $(2h_i/g)^{1/2}$, which is just less than a half of t_∞.

Further insight is obtained by an analysis of data on the radius of the flow front as a function of time, $r(t)$. For all flows there was a primary acceleration phase during which the acceleration was approximately constant between 0.25 g and 0.3 g. For $a < 1.7$ this acceleration phase was followed by a phase of deceleration which came quite abruptly to a halt. For $a > 1.7$ these two phases were separated by a phase of constant velocity of the flow front whose duration increased with increasing a. This phase of constant velocity has an analogue with the evolution of a fluid axisymmetric gravity current spreading at high Reynolds number, which also goes through a stage of constant velocity [14]. A fluid current then adjusts under a balance between buoyancy and inertial forces, spreading like $t^{1/2}$ [cf.(3.1)]—the same result as obtained for the granular collapse described here. This analogy, which uses quantitative relationships to describe the motion of the granular medium that are closely analogous to those used to describe the motion of density currents of Newtonian liquids, further strengthens our argument that intergranular frictional effects play a negligible role until the abrupt halt commences.

Obtaining the spreading relationships that our experiments have indicated remains a challenge for the future. A difficulty is that for at least half of the flow the concepts of shallow water theory, as applied by some to this problem, are false. In the meantime, a clue to understanding the emplacement we have observed may come from an interpretation of the final stages, when the spreading pile comes to a rapid halt. It has been suggested that granular materials can be considered in two states [43]: a static solid state, where intergranular forces at particle faces give the material strength; and a liquid state, exemplified by granular flows and fluidised beds, where the particles are in anagitated state and the system has negligible strength. The abrupt cessation of the motion of the granular flows that we observed can be likened to a phase change between two states [44]. In accord with the characterisation put forward in [45], the change of state can be envisaged as a kinetic process analogous to solidification of a true liquid. In the case of a granular medium, we suggest that as the flow decelerates, the granular temperature falls below a threshold value and frictional interactions between particles become dominant and the granular material converts to a static solid (or deposit).

Conclusions

Since the propagation and evolution of gravity currents was first quantitatively analysed more than sixty years ago, a lot has been determined. The rates of propagation under many different situations have been evaluated, as described in the various sections of this article. The subject area has seen considerable active research over the last thirty years or so, primarily due to the influence of the giant names in the subject, including von Karmen [2], Benjamin [3] and Simpson [45]. Part of the drive for the research has come from the natural applications to flows in the oceans, atmosphere, on the Earth surface and also deep within the Earth along particular phase boundaries [5,46] as well as to many engineering and industrial problems.

Acknowledgements

Many colleagues have helped me to understand the motion of gravity currents. I am grateful to each of them for their patience and wisdom.

References

[1] Turner, J.S. *Buoyancy effects in fluids*, Cambridge University Press 1979.

[2] Von Kármán, T. The engineer grapples with nonlinear problems, *Bull. M. Math. Soc.* **46**, 1940, 615–683.

[3] Benjamin, T.B. Gravity currents and related phenomena, *J. Fluid Mech.* **31**, 1968, 209–248.

[4] Huppert, H.E. The propagation of two-dimensional and axisymmetric viscous gravity currents over a rigid horizontal surface, *J. Fluid Mech.* **121**, 1982, 43–58.

[5] Huppert, H.E. The intrusion of fluid mechanics into geology, *J. Fluid Mech.* **173**, 1986, 557–594.

[6] Huppert, H.E. The flow and instability of viscous gravity

currents down a slope, *Nature* **300**, 1982, 427–429.

[7] Huppert, H.E. Geological Fluid Mechanics. In: *Perspectives in Fluid Dynamics: A Collective Introduction to Current Research*, eds. G. K. Batchelor, H.K. Moffatt and M.G. Worster. Cambridge University Press, 2000, 447–506.

[8] Huppert, H.E., Shepherd, J.B., Sigurdsson, H. and Sparks, R.S.J. On lava dome growth, with applications to the 1979 lava extrusion of Soufriere, St. Vincent, *J. Volcanol. and Geotherm. Res.* **14**, 1982, 199–222.

[9] Jaupart, C. Effects on compressibility on the flow of lava, *Bull. Volc.* **54**, 1991, 1–9.

[10] Fink, J.H. and Griffiths, R.W. Radial spreading of viscous gravity currents in solidifying crust, *J. Fluid Mech.* **221**, 1990, 485–510.

[11] Fink, J.H. and Griffiths, R.W. Morphology, eruption rates, and rheology of lava domes; insights from laboratory models, *J. Geophys. Res.* **103**, 1998, 527–548.

[12] McKenzie D., Ford, P.G., Liu, F. and Pettengill, G.H. Pancake-like domes on Venus, *J. Geophys. Res.-Planet* **97(E10)**, 1992, 15967–15976.

[13] Whitham, G.B. *Linear and Nonlinear Waves*, Wylie, 1974.

[14] Huppert, H.E. and Simpson, J.E. The slumping of gravity currents, *J. Fluid Mech.* **99**, 1980, 785–799.

[15] Harris, T. C., Hogg, A. J. and Huppert, H.E. A mathematical framework for the analysis of particle-driven gravity currents, Appendix A, *Proc. Roy. Soc. A* **457**, 2001, 1241–1272.

[16] Chen, J.C. Studies on gravitational spreading currents, PhD thesis, California Institute of Technology, 1980.

[17] Bonnecaze, R.T., Huppert, H.E. and Lister, J.R. Particle-driven gravity currents, *J. Fluid Mech.* **250**, 1993, 339–369.

[18] Bonnecaze, R.T., Hallworth, M.A., Huppert, H.E. and Lister, J.R. Axisymmetric particle-driven gravity currents, *J. Fluid Mech.* **294**, 1995, 93–121.

[19] Hallworth, M.A., Phillips, J., Huppert, H.E. and Sparks, R.S.J. Entrainment in turbulent gravity currents, *Nature* **362**, 1993, 829–831.

[20] Hallworth, M.A., Huppert, H.E., Phillips, J. and Sparks, R.S.J. Entrainment into two-dimensional and axisymmetric turbulent gravity currents, *J. Fluid Mech.* **308**, 1996, 289–312.

[21] Martin, D. and Nokes, R. Crystal settling in a vigorously convecting magma chamber, *Nature*, **332**, 1988, 534–536.

[22] Hallworth, M.A., Hogg, A.J. and Huppert, H.E. Effects of external flow on compositional and particle gravity currents, *J. Fluid Mech.* **359**, 1998, 109–142.

[23] Hogg, A.J., Huppert, H.E. and Hallworth, M.A. Constant flux currents in external mean flows. *J. Fluid Mech.* (sub judice).

[24] Hogg, A.J. and Huppert, H.E. Two-dimensional and axisymmetric models for compositional and particle-driven gravity currents in uniform ambient flows. In: Sediment Transport and Deposition by Particulate Gravity Currents. *Spec. Publs. int. Ass. Sediment* **31**, 2001, 121–134.

[25] Hogg, A.J. and Huppert, H.E. Spreading and deposition of particulate matter in uniform fluids, *J. Hydraul. Res.* **39(5)**, 2001, 505–518.

[26] Slim, A.C. Ph.D. thesis, Cambridge University, 2005.

[27] Huppert, H.E. Quantitative modelling of granular suspension flows, *Phil.Trans. R. Soc.* **356**, 1998, 2471–2496.

[28] Acton, J.M., Huppert, H.E. and Worster, M.G. Two-dimensional viscous gravity currents flowing over a deep porous medium, *J. Fluid Mech.* **440**, 2001, 359–380.

[29] Harris, T.C., Hogg, A.J. and Huppert, H.E. Polydisperse particle-driven gravity currents, *J. Fluid Mech.* **472**, 2002, 333–372.

[30] Thomas, L.P., Marino, B.M. and Linden, P.F. Gravity currents over porous substrait, *J. Fluid Mech.* **366**, 1998, 239–258.

[31] Ungarish, M. and Huppert, H.E. High-Reynolds-number gravity currents over a porous boundary: shallow-water solutions and box model approximations. *J. Fluid Mech.* **418**, 2000, 1–23.

[32] Maxworthy, T., Lielich J., Simpson, J.E. and Meiburg, E.H. Propagation of a gravity current in a linearly stratified fluid, *J. Fluid Mech.* **453**, 2002, 371–394.

[33] Ungarish M. and Huppert H.E. On gravity currents propagating at the base of a stratified ambient, *J. Fluid Mech.* **458**, 2002, 283–301.

[34] Griffiths, R.W. and Hopfinger, E. Gravity currents moving along a lateral boundary in a rotating fluid, *J. Fluid Mech.* **134**, 1983, 357–399.

[35] Griffiths, R.W. Gravity currents in rotating systems. *Ann. Rev. Fluid Mech.* **18**, 1986, 59–89.

[36] Hallworth, M. A., Huppert H. E. and Ungarish, M. Axisymmetric gravity currents in a rotating system: experimental and numerical investigations, *J. Fluid Mech.* **447**, 2001, 1–29.

[37] Ungarish, M. and Huppert, H.E. The effects of rotation on axisymmetric, particle-driven gravity currents, *J.Fluid Mech.* **362**, 1998, 17–51.

[38] Hallworth, M.A. and Huppert, H.E. Abrupt transitions in high-concentration, particle-driven gravity currents, *Phys. Fluids* **10**, 1998, 1083–1087.

[39] Griffiths, R.W. The dynamics of lava flows, *Ann. Rev. Fluid Mech.* **32**, 2000, 477–518.

[40] Mei, C.C., Liu, K.-F. and Yuhi, M. Mud flows - slow and fast, *Geormorphological Fluid Mech.* (eds): Balmforth, N. and Provencale, A., Springer-Verlag 2001, 548–577.

[41] Yuhi, M. and Mei, C.C. Slow spreading of fluid-mud over a conical surface, *J. Fluid Mech.* (in press).

[42] Lube, G., Huppert, H.E., Sparks, R.S.J and Hallworth, M.A. Axisymmetric collapses of granular columns, *J. Fluid Mech.* **508**, 2004, 175–199.

[43] Jaeger H.M., Nagel, S.R. and Behringer, R.P. Granular solids, liquids and gases, *Rev. Mod. Phys.* **68**, 1996, 1259–1273.

[44] Huppert, H.E. The fluid mechanics of solidification, *J. Fluid Mech.* **212**, 1990, 209–240.

[45] Simpson, J.E. *Gravity currents in the environment and the laboratory*, Cambridge University Press 1997.

[46] Kerr, R.S. and Lister, J.R. The spread of subducted lithospheric material along the mid-mantle boundary. *Earth Planet. Sci. Let.* **85**, 1987, 241–247.